MALAT1/miR-320a in bone marrow mesenchymal stem cells function may shed light on mechanisms underlying osteoporosis

Chengli Su[1], Hongning Wang[2], Luchen Xu[1], Yue Zhang[1], Yunfeng Li[1]

[1]State Key Laboratory of Oral Diseases, National Clinical Research Center for Oral Diseases, West China Hospital of Stomatology, Sichuan University, Chengdu, China
[2]Department of Orthodontics, Yantai Stomatological Hospital, Yantai, Shangdong Province, China

Corresponding author:
Yunfeng Li PhD
State Key Laboratory
of Oral Diseases
National Clinical
Research Center
for Oral Diseases
West China Hospital
of Stomatology
Sichuan University
No. 14, Section 3
South Renmin Road
Chengdu 610041, China
E-mail: doctorlyf@163.com

Abstract

Introduction: Growing evidence supports the involvement of long noncoding RNAs (lncRNAs) in bone metabolism and diseases. This study aims to investigate the involvement of the lncRNA metastasis-associated lung adenocarcinoma transcript 1 (MALAT1) in the pathological process of osteoporosis and the effects of MALAT1 on regulation of BMSC differentiation through competitive endogenous RNA (ceRNA) mechanisms.

Material and methods: The expression of MALAT1 and miR-320a was determined using RT-PCR in bone tissue derived from female SD (Sprague Dawley) rats with osteoporosis. Immunohistochemical (IHC) staining was used to evaluate the expression of neuropilin-1 (NRP-1) and β-catenin. Bone marrow mesenchymal stem cells (BMSCs) were divided into 4 groups: control, NC (negative control), MALAT1 siRNA, and miR-320a mimics. Forty-eight hours later, the effect of MALAT1 on the miR-320a expression, proliferation and osteogenic differentiation of BMSCs was investigated. Two weeks later, the cell activity, alkaline phosphatase (ALP) activity, and mRNA expression of Osterix and Runx2 were evaluated. Three weeks later, alizarin red staining of calcified nodules and Western blot analysis of the expression of β-catenin, NRP-1, osteocalcin (OCN), and osteopontin (OPN) were performed.

Results: Downregulated MALAT1 or upregulated miR-320a expression inhibited the activity and osteogenic differentiation of BMSCs, resulting in low ALP activity and NRP-1 expression, fewer calcified nodules, decreased mRNA levels of Osterix and Runx2, and inhibited expression of NRP-1, OCN, and OPN. MALAT1 silencing did not decrease the protein level of β-catenin in the cytoplasm but suppressed that in the nucleus.

Conclusions: Downregulated MALAT1 and upregulated miR-320a expression play an important role in the pathological process of osteoporosis, via inhibition of the osteogenic differentiation of BMSCs.

Key words: metastasis-associated lung adenocarcinoma transcript, miR-320a, osteoporosis, bone marrow mesenchymal stem cells, competitive endogenous RNA.

Introduction

There exist multiple risk factors in osteoporosis, for example age, bone mineral density (BMD), weight, bone geometry, caffeine [1, 2]. Osteopo-

_A M S_

rosis may occur when the rates of formation and apoptosis become imbalanced in the highly specialized osteoblasts and osteoclasts involved in bone maintenance [3]. Although there are many studies on the pathways involving osteoblast differentiation and bone formation, the interactions between osteogenesis-related signaling pathways remain unclear. Therefore, it is vital to find novel regulatory mechanisms upstream of the signaling pathways. Metastasis associated lung adenocarcinoma transcript 1 (MALAT1), located on chromosome 11q13.1, is a long noncoding RNA (lncRNA) with vital biological functions. It was found that RANKL inhibits the proliferation of osteoblasts by upregulating the expression of MALAT1 *in vitro* [4]. In addition, MALAT1 was found to regulate the expression of β-catenin, and the overexpression and down-regulation of MALAT1 can respectively induce and decrease the expression of β-catenin [5, 6]. However, the effect of lncRNA MALAT1 on bone metabolism function is poorly understood.

LncRNA refers to a large class of endogenous RNA molecules that do not encode proteins; noncoding RNAs include microRNA and long noncoding RNA, among others. LncRNAs can interact with a miRNA, regulate its downstream target genes and be adsorbed by a "sponge" to bind homologous miRNA molecules competitively with the target mRNA through a microRNA response element (MRE), resulting in a relative decrease in miRNA level and activity. This inhibits the silencing effect of a miRNA on its target mRNA; furthermore, the expression level of the target gene can be upregulated and the posttranscriptional level of the gene can be regulated by lncRNA in the "ceRNA" mechanism [7, 8]. Screening of microarray data revealed that the miRNA miR-320a was upregulated after knockdown of MALAT1 expression, while database and literature results showed that miR-320a can reciprocally interact with MALAT1 [9]. A literature investigation found that miR-320a was overexpressed in osteoporosis samples. miR-320a can target and inhibit CTNNB1, the gene of catenin β1, and subsequently inhibit lymphoid enhancer-binding factor 1 (LEF1) and RUNX2; therefore, it is considered that miR-320a has the effect of inhibiting osteogenesis differentiation [10]. The β-catenin gene was shown to be a direct target gene of miR-320a, and miR-320a negatively regulated the expression of β-catenin in cancer research [11]. In addition, studies have shown that miR-320a can target and inhibit the expression of NRP-1 [12].

A study found that inhibition of NRP-1 could affect the differentiation of osteoblasts by inhibiting the Wnt/β-catenin signaling pathway [13]. NRP-1, which is not only expressed on the surface of osteoclast precursors and osteoclasts but also expressed on the membrane of osteoblasts, plays a critical role in the molecular basis of Sema3A as a double regulator and modulator of bone [14, 15]. The NRP-1 and PlexinA1 receptor complex, which can implement cotransduction of intracellular signals after binding Sema3A, has the unique dual functions of promoting osteogenesis and inhibiting osteoclast differentiation, functions that are of great significance for promoting both bone formation and balancing bone metabolism [15]. Therefore, we speculate that MALAT1 may regulate the expression of NRP-1 and β-catenin by regulating miR-320a in the competing endogenous regulation mechanism.

The potential inherent involvement of MALAT1 in osteoporosis is investigated in the present investigation. In addition, we examined the mRNA expression level of miR-320a and MALAT1 in bone mesenchymal stem cells (BMSCs) derived from osteoporotic rats, and its effects on osteogenic differentiation and cell growth were tested. Furthermore, the underlying regulatory mechanism of the microRNA miR-320a in BMSCs were analyzed *in vitro*. Finally, the possible interaction between miR-320a and β-catenin, miR-320a and NRP-1 was also explored in BMSCs. The present investigation may promote better understanding of the regulatory mechanisms and correlations of MALAT1/miR-320a/NRP-1/β-catenin in osteogenesis *in vitro*.

Material and methods

Experimental animals

Female Sprague Dawley (SD) rats ($n = 51$), aged 3 months, weighing 226 ±22 g, were purchased from the Chengdu Laboratory Animal Center (Chengdu, China). From them, 48 female rats were divided into control ($n = 24$) and model ($n = 24$) groups at random, while 3 female rats were used for molecular experiments. Three animals were kept in each cage in a 25°C temperature-controlled room with 50–60% relative humidity and a 12 h light and 12 h dark cycle.

Establishment of the OVX animal models

After acclimatization for 2 weeks, following the intraperitoneal injection of ketamine (3B Scientific Corporation, USA) at a dose of 100 mg/kg, the rats underwent bilateral ovariectomy (OVX, $n = 24$) or sham surgery (Sham, $n = 24$). To obtain the tibial bone samples, the animals were sacrificed with euthanasia 3 months after the surgery.

BMSC isolation and primary cell culture

BMSCs were isolated from the femurs and tibiae of SD rats ($n = 3$), and we cultured the BMSCs according to previously reported methods [16].

Chengli Su, Hongning Wang, Luchen Xu, Yue Zhang, Yunfeng Li

Cells were incubated in 5% CO_2 in 95% humidity at 37°C. The culture media consisted a rate of 10 : 1 : 0.1 minimum essential medium α medium (α-MEM, Gibco, USA), 10% fetal bovine serum (FBS, Gibco, USA), and penicillin-streptomycin (Gibco, USA). When adherent cells reached 90% confluence, the cells were treated with a 0.25% trypsin solution for continued passage. BMSCs, derived from the third generation, were prepared for the subsequent experiments. The transfected BMSCs for each group were grown for approximately 7 days, and the culture wells were supplemented with osteogenesis inducing conditional medium. Osteogenic induction medium contains 500 ml of α-MEM, 50 g/ml ascorbic acid, 10^{-8} M dexamethasone, and 8 mM β-glutamine.

Hematoxylin and eosin (HE) staining and micro-computed tomography (micro-CT) scanning

The tibial metaphyseal bone of ovariectomy and sham-operated rats was fixed with 10% polyformaldehyde. The tibial metaphyseal bone underwent 5% nitric acid decalcification, washing with flowing water, routine dehydration, and xylene permeabilization. Tibial axis sections (5 μm) were obtained, hematoxylin and eosin staining was performed, a neutral resin seal sheet was applied, tissue sections were observed under an optical microscope to analyze the morphology of the bone and tissue, and microarchitecture of the

Table I. PCR primers used for PCR

Genes	Primers
GAPDH	Forward: 5′-GATGACATCAAGAAGGTGGTGA-3′
	Reverse: 5′-GATGACATCAAGAAGGTGGTGA-3′
MALAT1	Forward: 5′-GTTACCAGCCCAAACCTCAA-3′
	Reverse: 5′-CTACATTCCCACCCAGCACT-3′
RUNX2	Forward: 5′-CCTATGACCAGTCTTACCCC-3′
	Reverse: 5′-CAGAGGCAGAAGTCAGAGGT-3′
Osterix	Forward: 5′-CTTACCCGTCTGACTTTGCC-3′
	Reverse: 5′-CGCTCTAGCTCCTGACAGTT-3′

Table II. Paired primers of siRNAs and NC

siRNA	Primers
NC	Forward: 5′-UCUCCGAACGUGUCACGUTT-3′
	Reverse: 5′-ACGUGACACGUUCGGAGATTT-3′
MALAT1 siRNA-1	Forward: 5′-GCUCAGGACUUUGCAUAUATT-3′
	Reverse: 5′-UAUAUGCAAAGUCCUGAGCTT-3′
MALAT1 siRNA-2	Forward: 5′-CAGAAGAGUUGCUUCAUUTT-3′
	Reverse: 5′-AAUGAAGCAACUCUUCUGCTT-3′
MALAT1 siRNA-3	Forward: 5′-CGGAAUUGCUGGUAGUUUTT-3′
	Reverse: 5′- AAACUACCAGCAAUUCCGCTT-3′

proximal rat tibiae was examined by micro-computed tomography (micro-CT) scanning by a CT scanner (Scanco Medical, Bassersdorf, Switzerland) to determine whether the model of osteoporosis was successful. The resolution for the slices was 2048 × 2048 pixels, and the isotropic voxel size was 10 μm. A CT system (70 kV, 114 μA; μ-CT 80 scanner) was used to scan the volume of interest. To evaluate the bone morphometric parameters to the proximal tibial metaphysis, we defined the volume of interest (VOI) as the distal slices ($n = 100$) from the proximal tibial growth plate.

Quantitative reverse transcription polymerase chain reaction (RT-PCR) assays

Quantitative RT-PCR was used to determine the level of miR-320a and MALAT1 in the bone tissue of each group; MALAT1 siRNA interference efficiency, transfection efficiency, and mRNA expression in Osterix and Runx2 were also evaluated.

To explore the expression levels of miR-320a and MALAT1 in the bone tissue of the osteoporosis group and the control group, tibial bones of the ovariectomy and control groups were harvested 3 months after the ovariectomy or sham surgery. The tibial metaphysis was placed in a TRIzol (1 ml) (Gaithersburg, MD) homogenate tube for shredding and grinding to extract the total RNAs; according to the instructions of the manufacturer, RNA was extracted step by step and used for amplification. The subsequent steps included denaturation and amplification.

After 14 days of osteogenic induction, the cultured and harvested BMSCs were flushed with TRIzol reagent (1 ml) (Gaithersburg, MD), and the RNA and reaction system was prepared according to the manufacturer's specification. Melting curve analysis was performed after the process of amplification and the subsequent fluorescence measurements. For the quantification of all mRNA expression levels, control wells without cDNA were induced for analysis using the $2^{-\Delta\Delta Ct}$ method to analyze the fold changes in miRNA or the related gene expression changes in each sample. The primer (Carlsbad, CA, USA) sequences, including the sequence for MALAT1, RUNX2, Osterix, miR-320a and U6, used for RT-PCR are listed in Table I (when GAPDH was used for normalization of data).

Small interfering RNA

Three kinds of small interfering RNAs (siRNA) targeting MALAT1 and miR-320a mimics and the negative control were prepared by 100BIOTECH (Hangzhou, China). They were transfected to BMSCs with Lipofectamine 2000 reagent according to the manufacturer's instructions. Table II lists the primer sequences of the siRNA and control

siRNA for MALAT1. The process of transfection of siRNA into BMSCs is based on the manufacturer's instructions. New medium was added to the cells after transfection for 24 h, and the *in vitro* interference efficiency of four groups of siRNA was determined by qRT-PCR.

Immunohistochemical (IHC) analysis

The paraffin-embedded tissue samples (tibial bone from ovariectomy and sham surgery rats) were examined to determine the protein expression of NRP-1 and β-catenin. Specimens were blocked with 4% paraformaldehyde (24 h) and decalcified in 10% EDTA (Nanjing BaiRui Biotechnology Co. Ltd.) solution (1 month). After gradient ethanol dehydration and baking, paraffin sections were obtained. Sections were heated to a boil, then heated at low heat for 20 min for antigen retrieval. Sections were placed in 3% H_2O_2 solution and incubated at room temperature for 10 min to block endogenous peroxidase. Then, sections were washed 3 times with PBS (5 min each time), dried and blocked in 5% BSA for 20 min. After the removal of BSA liquid, 50 μl of primary antibody diluted against NRP-1 and β-catenin (rat polyclonal anti-NRP-1 antibody 1 : 250, rat polyclonal anti-β-catenin antibody 1 : 500, Boster, Wuhan, China) was added to each section, and the tissues was covered at 4°C overnight. The rat peroxidase-diaminobenzidine kit (Maixin_Bio, Fuzhou, China) was used in this experiment. To each slice 50–100 μl of biotinylated second antibody (goat anti-rat, dilution ratio 1 : 1000) of the corresponding species was added. Each section received 50–100 μl of freshly prepared DAB solution (Beyotime, Suzhou, China), stained with hematoxylin, rinsed and turned blue. The cells that stained brown were regarded as positive cells. Five high power microscopic fields were selected from each section from the inverted fluorescence microscope to count positive cells at random, and finally the average value was obtained.

Osteogenic differentiation induction

After transfection, the BMSCs in each group grew for approximately 7 days, the osteogenic induction medium (containing 500 ml of α-MEM, 50 g/ml ascorbic acid, 10^{-8} M dexamethasone, and 8 mM β-glutamine), obtained from Sigma (St. Louis, MO), was added to the culture wells. The alkaline phosphatase (ALP) activity of osteoblasts was determined by using an alkaline phosphatase kit after 14 days of induction.

CCK-8 kit assay

A CCK-8 Kit (Beyotime, Suzhou, China) was used to determine the changes in cell activity in each group on the 14th day after culture. Ten microliters of CCK-8 solution was added to each well for each group at 37°C and 2 h, the sample was incubated with 5% CO_2, and the OD values were calculated at 450 nm with ELISA (BioTek, USA) on the 14th day of culture.

Alkaline phosphatase (ALP) activity

The ALP activity of osteoblasts was determined by an ALP kit 14 days after induction. The working solution of the standard product was prepared with 15 μl of p-nitrophenol phosphate (pNPP) solution (10 mM) and was diluted to 0.3 ml to reach a final concentration 0.5 mM. The ALP activity was calculated by using the OD value at 405 nm per milligram of total protein. All the experiments were conducted in triplicate.

Alizarin red staining

Each group of BMSCs grew for approximately 7 days, and culture wells were supplemented with the osteoblast-inducing medium. The culture medium was replaced every 2 days to observe the growth and calcification of the osteoblasts. After 21 days of continuous culture, alizarin red staining was performed to evaluate the calcium deposition/mineralization of osteoblasts. The culture supernatant was washed with PBS 3 times. Alizarin Red S dye solution (Wuhan, China) was added at 37°C. The microscope was used to obtain images and records of the plates.

Western blot assay

Each cell sample was divided into two parts and one part was used to determine the expression of β-catenin protein by using a cytoplasmic and nuclear isolation kit to extract cytoplasmic and nucleoproteins, respectively. Total protein was collected to determine the quantitative protein levels of neuropilin-1 (NRP-1), osteocalcin (OCN), and osteopontin (OPN). BCA quantification was performed strictly according to the instructions of a BCA protein concentration assay kit. The membrane was sealed with secondary antibody (10% goat serum). Primary antibody (1 : 1000, rat anti-NRP-1, OCN, OPN IgG, Beyotime, China) was added to the membrane and incubated for 1 night at 4°C. After being washed with PBS three times, the secondary antibody (1 : 4000, goat anti-rat antibody, Beyotime, China) was added to the membrane and incubated at 37°C for 1 h.

Statistical analysis

Data were analyzed by SPSS 16.0 (SPSS, Chicago, IL), and the results are expressed as the

Chengli Su, Hongning Wang, Luchen Xu, Yue Zhang, Yunfeng Li

mean ± SD. In the animal study, specimens were harvested from 48 different rats for each group. For cell analysis, all experiments were repeated 3 times in triplicate. $p < 0.05$ indicated a statistically significant difference. Comparison between two groups was performed using the *T*-test, and comparison among four groups was conducted by one-way ANOVA.

Results

Evaluation of the bone specimens from OVX and sham-operated rats

Tibia specimens were harvested from OVX and sham-operated groups 3 months after the operation. The pathological changes in the tibia examined by using histological sections and micro-CT scanning confirmed the establishment of osteoporosis (Figures 1 A, B). The trabeculae of the sham-operated group were uniform in size, arranged and connected into a net. In the OVX group, the trabeculae were broken, the structures were distorted and loosely arranged, and most of them could not be connected into a network (Figure 1 A). Quantitative micro-CT analysis showed an obvious decrease in percent bone volume, as well as damaged bone microarchitecture, in the OVX group compared to that in the control group (Table III). The trabecular separation for OVX rats increased 380% compared with the sham operated groups ($p < 0.01$, Table III). Compared with the sham operated groups, Tb·Th decreased by 46.1% ($p < 0.05$) and Tb·N decreased by 69.6% ($p < 0.05$, Table III). RT-PCR results showed that the MALAT1 expression in the bone tissue of the OVX group was decreased by 85.6% ($p < 0.05$) (Figure 1 C), while the expression of miR-320a was increased by 82.9% ($p < 0.01$) compared to that of the control (Figure 1 D). The IHC staining showed more positive brown color in the femur of rats in each sham operated group, and the IHC results showed inhibited expression of NRP-1 and β-catenin in OVX rats compared to that in the control (Figure 1 E). The number of NRP1 positive cells expressed in the osteoporotic group compared with the control group was significantly decreased ($p < 0.05$, Table IV). Compared with the control group, the positive number of β-catenin expressed in the osteoporotic group was significantly decreased ($p < 0.05$, Table IV).

Effects of MALAT1 interference on miR-320a expression and cell activity in BMSCs

After transfection for 48 h, the transfection efficiency of MALAT1 siRNA and miR-320a mimics was confirmed by RT-PCR evaluation (Figures 2 A, B). According to Figure 2 A, we found that MALAT1 siRNA-1 had the best interference efficiency, so we

selected MALAT1 siRNA-1 for our further experiments (Figure 2 A).Compared to the control group, the group with MALAT1 interference had increased expression of miR-320a (Figure 2 B), while overexpression of miR-320a showed no effect on the MALAT1 level (Figure 2 A). The CCK8 test was conducted after transfection for 14 days. Compared to cells cultured in ordinary medium, the cells in osteogenic medium had increased cell activity; for osteogenesis induced cells, gene transfection of MALAT1 siRNA and miR-320a mimics decreased the cell activity, as shown by the CCK-8 kit results 14 days after osteogenic induction.

ALP activity, RT-PCR, and calcified nodule evaluation of osteogenic differentiation of BMSCs

Fourteen days after inducing culture, the ALP activity of induced BMSCs in the MALAT1 siRNA group and the miR-320a mimic group was decreased by 60.9% and 66.4% respectively, compared to that in the control ($p < 0.01$); the above results showed that Malat1 siRNA group and miR-320a mimics had weaker bone formation ability compared with control group (Figure 3 A). The expression of Osterix was decreased by 53.2% ($p < 0.01$) in the MALAT1 group and by 46% ($p < 0.05$) in the miR-320a mimics group (Figure 3 B). The expression of Runx2 was decreased by 83% in the MALAT1 siRNA group ($p < 0.01$) and by 70.5% in the miR-320a mimics group ($p < 0.01$) compared to that in the control group (Figure 3 C). As a measure of critical functions in the mature osteoblasts, the matrix mineralization and calcium deposition levels were evaluated by Alizarin red staining under an inverted microscope after 21 days of osteogenetic induction. The number of orange calcified nodules observed in the MALAT1 siRNA group and miR-320a mimics group decreased significantly compared with that in the control group (Figure 3 D).

Western blot assay of β-catenin, NRP-1, OCN and OPN in BMSCs

The cytoplasm and nuclear fraction of β-catenin protein were extracted by cytoplasm and nuclear isolation kits, respectively, and then evaluated by a Western blot assay (Figure 4 A). The β-catenin level in the cytoplasm showed no difference, but that in the nucleus decreased significantly in the MALAT1 siRNA and miR-320a mimics groups. The ratio of the nuclear to cytoplasmic β-catenin in the MALAT1 siRNA group and the miR-320a mimics group showed significant downregulation by 65.1% ($p < 0.01$) and 72.2% ($p < 0.01$) compared to that in the control (Figure 4 B). NRP-1, OCN and OPN were also measured by Western blotting af-
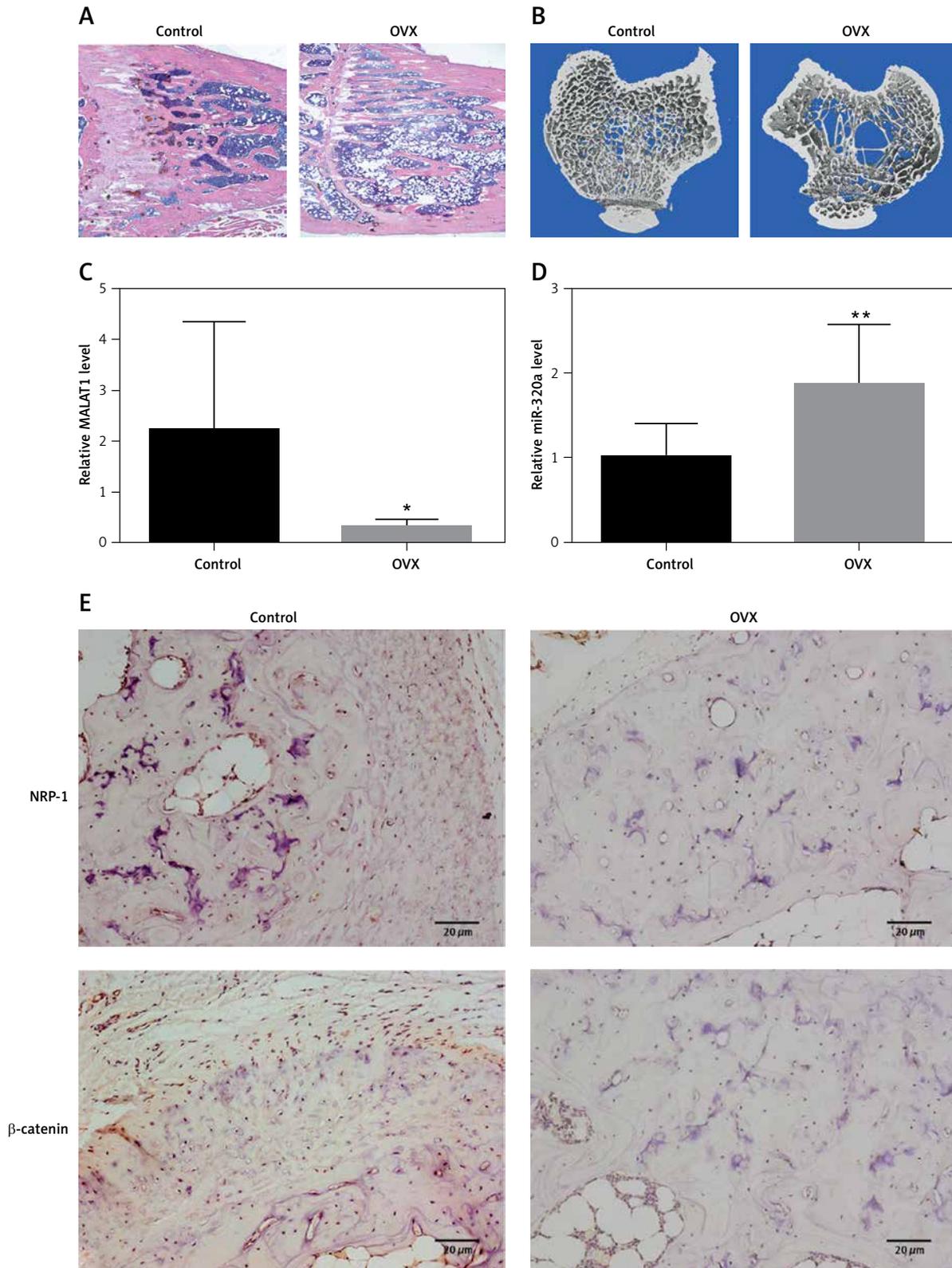
Figure 1. A – HE staining results of the tibial metaphyseal bone obtained from ovariectomy and sham surgery rats (*n* = 24). **B** – Images from micro-CT scanning of the proximal tibia in osteoporotic and intact SD rats; a significant reduction in the number of trabeculae and a decrease in the continuity of bone trabeculae can be seen in the osteoporosis group. **C**, **D** – Expression levels of miR-320a and MALAT1 were determined by qRT-PCR, and significantly reduced expression of MALAT1 and overexpression can be seen in Figure 1 C and 1 D. **E** – Protein expression of NRP-1 and β-catenin was determined by immunohistochemistry. Scale bar = 20 μm (*p < 0.05, **p < 0.01 compared with control)

Table III. Parameters used in micro-CT to evaluate microstructure changes in tibia

Microstructure parameter	Sham-operated	OVX
BV/TV	0.43 ±0.12	0.13 ±0.08**
Tb·Sp [mm]	0.21 ±0.04	1.01 ±0.09**
Tb·Th [1/mm]	0.13 ±0.03	0.07 ±0.01**
Tb·N [1/mm]	3.45 ±0.41	1.05 ±0.22**

Table IV. Number of NRP1-positive and β-catenin-positive cells after immunohistochemistry in the tibia (1000×)

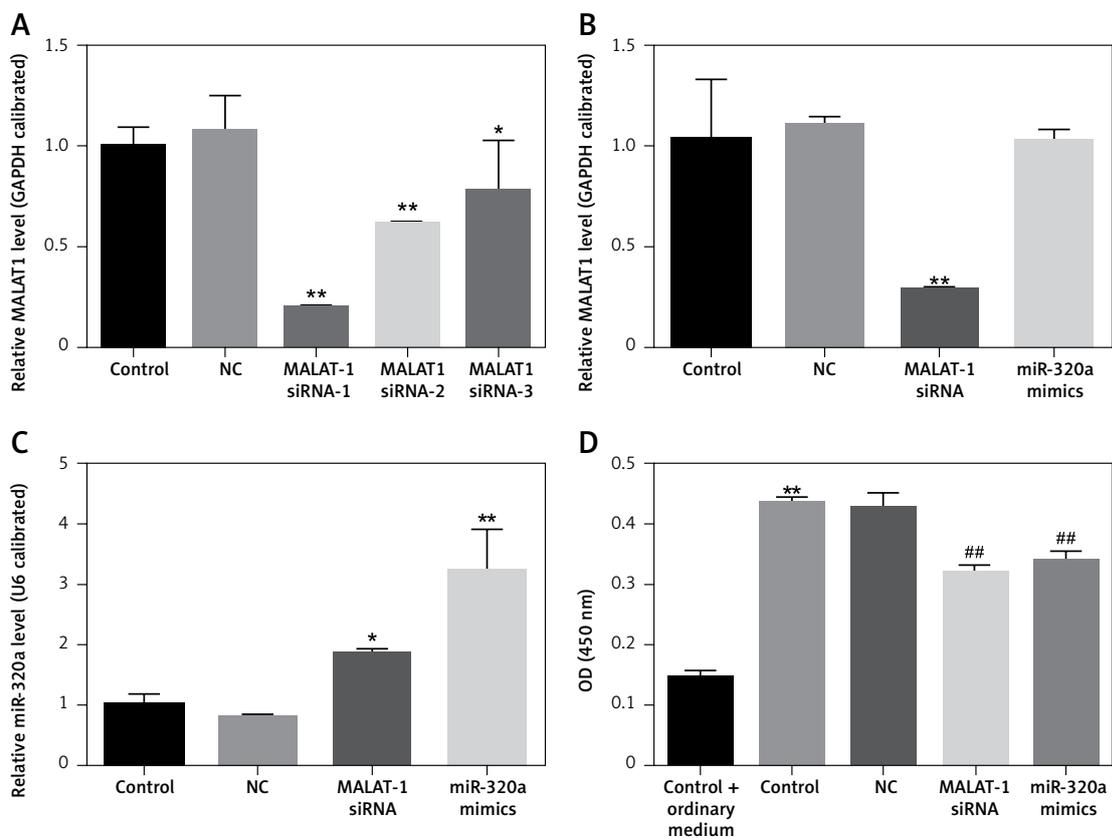| Group	N	Control	Model	P-value
NRP1	24	31.3 ±5.2	13.6 ±3.1	0.021
β-catenin	24	29.7 ±4.7	10.1 ±1.4	0.017

Figure 2. A – MALAT1 level in BMSCs was determined by qRT-PCR after transfection with the vector, MALAT1 siRNA-1, MALAT1 siRNA-2 and MALAT1 siRNA-3 for 48 h. MALAT1 siRNA-1 showed the best transfection efficiency and can be used for further study. The MALAT1 level (**B**) and the miR-320a level (**C**) in BMSCs were determined by qRT-PCR after transfection with the vector, MALAT1 siRNA-1, and miR-320a mimics for 48 h. **D** – Activity of BMSCs was observed via a CCK-8 assay after osteogenesis was induced with osteogenic induction medium for 14 days. The groups in the CCK-8 test were divided into the following groups: 1) Control + ordinary medium: blank control + culture media; 2) Control: blank control + osteogenic induction medium; 3) NC: vectors + osteogenic induction medium; 4) MALAT1 siRNA: MALAt1 siRNA1 transfection + osteogenic induction medium; 5) miR-320a mimics: miR-320a mimics transfection + osteogenic induction medium (*$p < 0.05$, **$p < 0.01$ compared with control)

ter 21 days of osteogenic induction (Figure 4 C). The results demonstrated that the expression of NRP-1, OCN and OPN protein was significantly decreased in the MALAT1 siRNA group compared to that in the control by 36.8% ($p < 0.01$), 35.6% ($p < 0.05$) and 23.1% ($p < 0.05$) respectively. Similarly, the expression of NRP-1, OCN and OPN protein in the miR-320a mimics group also decreased by 53.4% ($p < 0.01$), 42.9% ($p < 0.05$) and 21.2% ($p < 0.05$), respectively, compared to that in the control group (Figures 4 D–F).

Discussion

There may be a correlation between osteoporosis and other diseases such as left ventricular hypertrophy (LVH) [17]. Osteoporosis mainly results
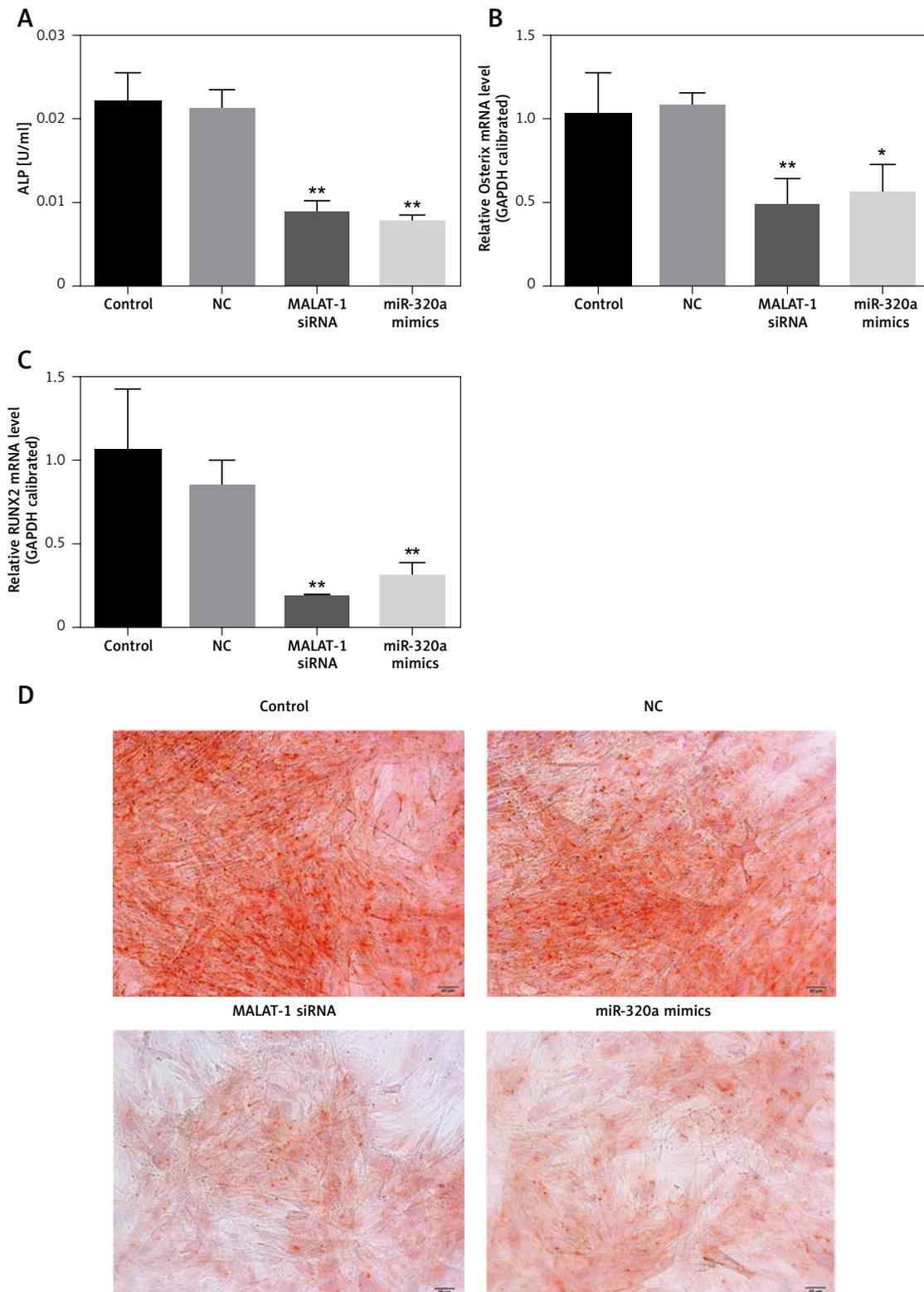
Figure 3. A – ALP activity of osteoblasts was determined by alkaline phosphatase kit 14 days after osteogenesis induction in BMSCs (ALP: alkaline phosphatase), and the activity of ALP in the MALAT1 siRNA group and miR-320a mimics group was significantly decreased ($p < 0.01$). The expression of Osterix (**B**) and RUNX2 (**C**) was determined by qRT-PCR after osteogenesis was induced in BMSCs for 14 days (RUNX2: Runt-related transcription factor 2). **D** – Alizarin red staining was conducted to observe the formation of calcified nodules under an inverted microscope after BMSC osteogenesis was induced for 21 days; a large number of calcified nodules were observed in the control group and NC group compared with the MALAT1siRNA group and miR-320a mimics group, and the number of calcified nodules in the cells of the MALAT1 siRNA group and miR-320a mimics group was significantly decreased. Scale bar = 20 µm (*$p < 0.05$, **$p < 0.01$ compared with control)

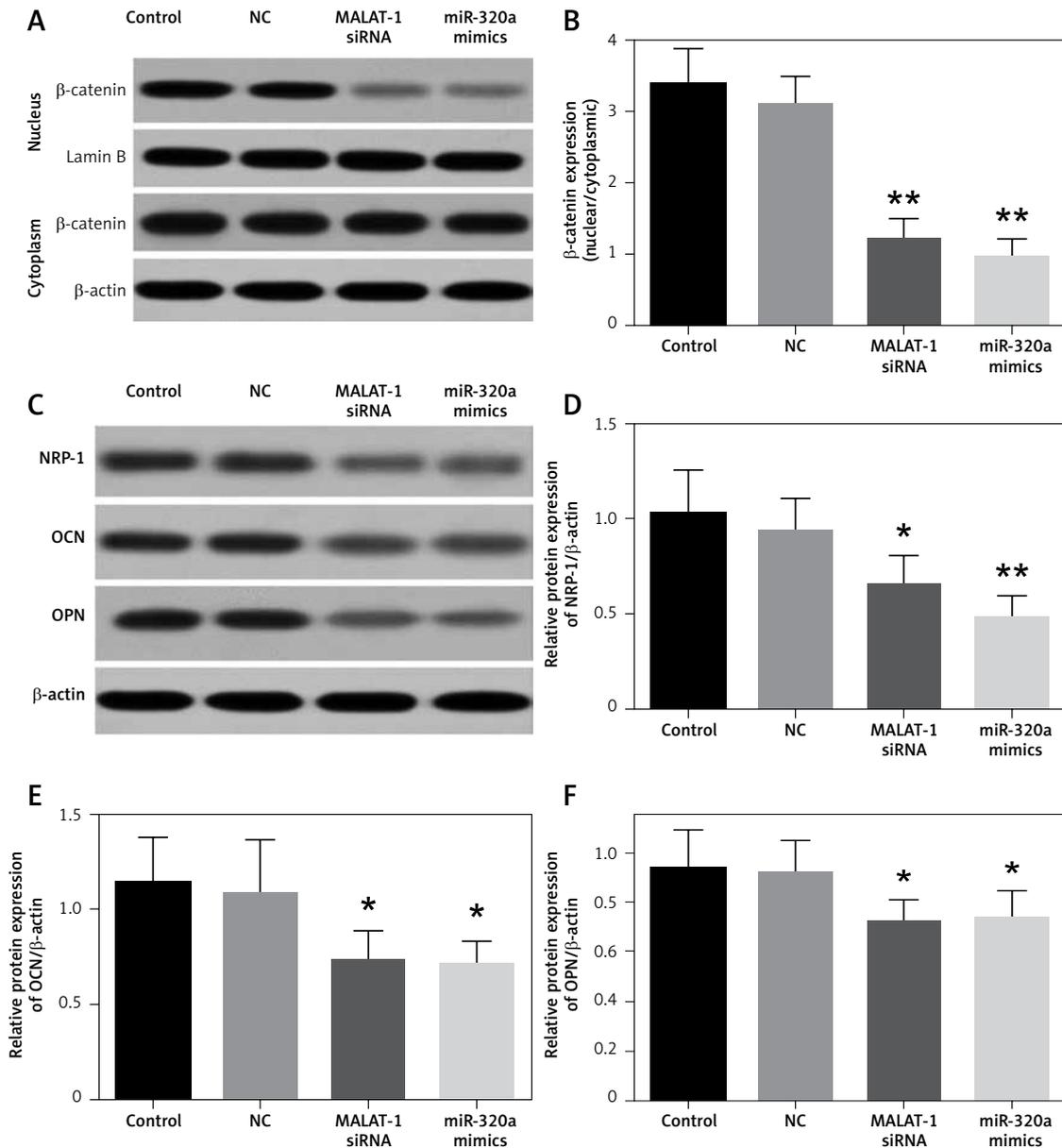Chengli Su, Hongning Wang, Luchen Xu, Yue Zhang, Yunfeng Li

Figure 4. A – Protein level of β-catenin in the cytoplasm and nucleus was determined by Western blot; β-catenin expression was observed to be significantly decreased in MALAT1 siRNA and miR-320a mimics groups in the nucleus. **B** – The ratio of β-catenin in the nucleus to that in the cytoplasm was calculated and compared between groups (**$p < 0.01$ compared with control). **C–F** – Western blot analysis was used to identify the osteogenic differentiation of BMSCs in different groups, by evaluation of the protein levels of NRP-1, OCN, and OPN (NRP-1 – neuropilin-1; OCN – osteocalcin; OPN – osteopontin) (*$p < 0.05$, **$p < 0.01$ compared with control)

from an imbalance between osteoblastogenesis and osteoclastogenesis. The process in which osteoblasts are derived from multipotent MSCs plays a critical role in the development of osteoporosis and involves a complex of molecules that mediate cell-matrix and cell-cell interaction [3]. Over time, studies focused on the underlying regulatory mechanism of osteoporosis have shifted from protein-coding RNA to noncoding RNAs.

LncRNAs, which mediate epigenetic modifications of DNAs but do not encode proteins, are a group of transcripts that are more than 200 nucleotides long [18]. The evidence for lncRNAs in osteoporosis is accumulating, and lncRNA are believed to be involved in the osteoblastic differentiation [19]. Moreover, 59 differentially expressed lncRNAs were found to be upregulated and 57 were downregulated between untreated and BMP2-treated groups of MSCs undergoing osteoblast differentiation [20]. However, the underlying role that lncRNA plays in osteoporosis remains to be further delineated. In previous studies, the lncRNA MALAT1 was found to be upregulated in osteoblast cells *in vitro*; the lncRNA MALAT1 was

closely related to the process of RANKL binding to the receptor RANK, and MALAT1 expression can be induced by RANKL [4].

An experiment showed that local use of medicine at the site of post-menopausal osteoporosis *in vivo* helped to promote the osseointegration [21]. It has been reported that MALAT1 can directly interact with miR-204 and functions as a miRNA sponge to positively regulate the osteogenic differentiation involved in CAVD (calcific aortic valve disease) pathogenesis [22]. Nevertheless, little is clear about the function of MALAT1 in osteoporosis and the underlying role of MALAT1 in bone metabolism. In the present study, we focus on MALAT1, which was investigated in cancer and tumor and is known as a noncoding RNA that is spliced infrequently. Through a rat model of osteoporosis, we observed that the level of MALAT1 in bone tissue was dramatically decreased in osteoporotic rats compared with that in control rats. We found that the osteoblasts induced from transfected BMSCs treated with MALAT1-siRNA showed significant inhibition of cell viability, calcium nodule formation, alkaline phosphatase activity and deposition of calcium nodules. Therefore, we further speculated that MALAT1 has an effect on osteogenic differentiation in bone metabolism and that the increase of MALAT1 in BMSCs may be related to the development of osteoporosis.

miRNAs are approximately 22 nucleotides long and can exert a silencing effect by mediating posttranscriptional modification to regulate the process of generating protein from mRNA [23]. MicroRNAs have critical roles in different diseases, they can mediate the metabolism of statins through the way of inflammation modulation and immune regulation in cardiovascular disease (CVD) [24]. MicroRNAs are new promising therapeutic targets for heart failure and familial hypercholesterolemia (FH) patients [25, 26]. It has been emphasized that abnormalities in the network of microRNA signaling may promote both the development and progression of osteoporosis, and, more importantly, miRNAs are emerging as crucial modulators of bone mass maintenance in osteoporosis [27]. However, further work to validate the underlying mechanisms before making definitive conclusions is required. A recent review highlighted both the advantages and challenges of using miRNAs in the circulating system as potential biomarkers, such as in patients with bone disease [28]. Competitive endogenous RNA (ceRNA) has specific mechanisms for regulating the influence of long noncoding RNAs (lncRNAs) on mRNAs levels by competing for a limited pool of microRNAs [29]. miRNAs act mainly to control gene downregulation by silencing the mRNA translation process after a specific sequence binds to its target gene through microRNA recognition elements (MRE),

and miRNAs may also bind lncRNA species [8, 29]. MALAT1 can act as a miRNA sponge to regulate the expression of target miRNAs (including miR-320a) and protein-coding genes as a hypothetical type of competitive endogenous RNA (ceRNA) [9]. A recent study proved that upregulation of the microRNA miR-320a can negatively regulate the levels of MALAT1 and that miR-320a can reciprocally interact with MALAT1 [9]. However, it remains to be elucidated whether MALAT1 can regulate miR-320a to promote osteoblast differentiation from BMSCs through the ceRNA mechanism *in vitro*.

Dramatically increased MALAT1 expression was observed in osteoporotic rats compared to that in control rats in bone tissue examined by qRT-PCR. According to the present research, miR-320a was identified as a suppressor that inhibited the proliferation and osteogenic differentiation of BMSCs. Here, it was found that the level of miR-320a was significantly upregulated in BMSCs with MALAT1 silencing, but no obvious expression change in MALAT1 was found in the miR-320a mimics group; that is, the downregulation of MALAT1 can upregulate the level of miR-320a in BMSCs. However, the increase in miR-320a had no significant effect on the MALAT1 expression in BMSCs. Furthermore, the same phenomenon was observed in the BMSCs of the miR-320a mimics group. The increased miR-320a level in BMSCs also inhibited the activity of osteoblasts, the deposition of calcium nodules and the activity of alkaline phosphatase, which we had observed in the MALAT1 siRNA group *in vitro*. In other words, we proved that MALAT1 repression regulates the osteogenic differentiation of BMSCs through an effect mediated by miR-320a, which is mediated by the ceRNA mechanism. However, whether proteins and osteoblast-related pathways are involved in the differentiation process that is regulated by ceRNA remained unclear. Therefore, we further investigated some key proteins and pathways related to osteogenesis.

Previous studies have shown that OPG promotes bone formation through inhibiting bone resorption and RANKL inhibition in an OVX rat models [30]. Runx2 is upregulated first, followed by Osterix, and ALP, OCN, and OPN are then upregulated as late protein markers [31]. We found that decreasing MALAT1 or increasing miR-320a can inhibit the osteogenic differentiation of rat BMSCs by inhibiting the mRNA level of Runx2 and Osterix, as determined by RT-PCR. OPN can be produced by cells such as preosteoblasts and osteoblasts and plays major roles in bone morphogenesis, immunoregulation and inflammation [32]. One study reported that the increase in OCN was associated with an increased level of new bone formation and osteocalcin, an early marker of osteogenesis, in rat mesenchymal stem cells [31, 32]. Our *in vitro*

Chengli Su, Hongning Wang, Luchen Xu, Yue Zhang, Yunfeng Li

evaluation of OCN and OPN verified that the decrease in osteogenic activity of BMSCs could be due to an increased level of miR-320a resulting from the decrease in the MALAT1 level.

NRP-1 and Sema3A binding can stimulate the differentiation of osteoblasts or inhibit the differentiation of osteoclasts respectively, through the canonical Wnt/β-catenin signaling pathway, and these effects are mediated by the receptor activator of nuclear factor-κB ligand (RANKL) secreted by osteoblasts [15]. It has been found that miR-320 can negatively regulate the expression of NRP-1 through regulating the target gene of NRP-1, contributing to the proliferation and migration of CCA cells [12]. We confirmed that the knockdown of MALAT1 significantly inhibited the expression of NRP-1 protein through the ceRNA mechanism *in vitro*. Canonical Wnt/β-catenin signaling plays a critical role in the regulation of bone homeostasis, while activation of this signaling can lead to increased bone mass and strength and is an intervention target for restoring mineral density [33]. The β-catenin signaling pathway positively regulates osteoblasts by activating T cell factor (TCF)-dependent transcription [34]. Studies have found that upregulated MALAT1 can modulate Wnt/β-catenin signaling to inhibit oral tongue squamous cell apoptosis. Furthermore, evidence has shown that downregulation of the lncRNA MALAT1 can decrease β-catenin expression in esophageal cancer cells *in vitro* [6]. β-Catenin can target miR-320a directly, and β-catenin overexpression is associated with low expression of miR-320a in glioblastoma multiform (GBM) cells [35]. In addition, it has been proved that β-catenin can target and regulate miR-320a directly in colon cancer cells [27].

The results of the experiment show a decrease of MALAT1 in osteoporotic rats, which is consistent with the decrease of osteogenic differentiation in rats after interfering with MALAT1. Therefore, we speculate that the intervention of MALAT1 can regulate the osteogenic differentiation of BMSCs in osteoporotic patients. This experiment is helpful to understand the potential regulatory mechanism of osteoporosis patients. MALAT1 may be a potential target for the treatment of osteoporosis.

In the present research, we found that a decrease of MALAT1 or an increase in miR-320a significantly reduced the nuclear β-catenin in osteoblasts; however, there was no reduction in the cytoplasm. It can be speculated that the distinct difference in inhibitory effects between the cytoplasm and nucleus may be related to the location of MALAT1, which is a common phenomenon in the "competitive endogenous RNA" hypothesis, where a preferential competitive combination exists in neighboring connections. In general, we speculate that due to the low expression of MALAT1, miR-320a upregulation followed the

downregulation of β-catenin and NRP-1 expression through the mechanism of ceRNA, leading to the osteogenic differentiation inhibition of BMSCs in osteoporosis patients. More importantly, our study may open the road to new gene regulatory networks acting through miRNA-lncRNA competitive interactions in osteoporosis. We first demonstrated that NRP-1 and β-catenin can be functionally targeted by miR-320a directly in BMSCs and highlighted the potential value of lncRNA MALAT1 and miR-320a as promising targets for a novel treatment of osteoporosis.

In conclusion, this knowledge of MALAT1/miR320a in BMSC function may shed light on mechanisms underlying osteoporosis. The upregulated miR-320a expression may result from the down-regulated MALAT1 expression, which can be explained by the ceRNA mechanism.

Acknowledgments

Conflict of interest

The authors declare no conflict of interest.

References

1. Dytfeld J, Marcinkowska M, Drweska-Matelska N, Michalak M, Horst-Sikorska W, Slomski R. Association analysis of the COL1A1 polymorphism with bone mineral density and prevalent fractures in Polish postmenopausal women with osteoporosis. Arch Med Sci 2016; 12: 288-94.
2. Lo HC, Kuo DP, Chen YL. Impact of beverage consumption, age, and site dependency on dual energy X-ray absorptiometry (DEXA) measurements in perimenopausal women: a prospective study. Arch Med Sci 2017; 13: 1178-87.
3. Manolagas SC. Birth and death of bone cells: basic regulatory mechanisms and implications for the pathogenesis and treatment of osteoporosis. Endocr Rev 2000; 21: 115-37.
4. Che W, Dong Y, Quan HB. RANKL inhibits cell proliferation by regulating MALAT1 expression in a human osteoblastic cell line hFOB 1.19. Cell Mol Biol 2015; 61: 7-14.
5. Liang J, Liang L, Ouyang K, Li Z, Yi X. MALAT1 induces tongue cancer cells' EMT and inhibits apoptosis through Wnt/beta-catenin signaling pathway. J Oral Pathol Med 2017; 46: 98-105.
6. Wang W, Zhu Y, Li S, et al. Long noncoding RNA MALAT1 promotes malignant development of esophageal squamous cell carcinoma by targeting beta-catenin via Ezh2. Oncotarget 2016; 7: 25668-82.
7. An Y, Furber KL, Ji S. Pseudogenes regulate parental gene expression via ceRNA network. J Cell Mol Med 2017; 21: 185-92.
8. Martirosyan A, De Martino A, Pagnani A, Marinari E. ceRNA crosstalk stabilizes protein expression and affects the correlation pattern of interacting proteins. Sci Rep 2017; 7: 43673.

9. Sun JY, Zhao ZW, Li WM, et al. Knockdown of MALAT1 expression inhibits HUVEC proliferation by upregulation of miR-320a and downregulation of FOXM1 expression. Oncotarget 2017; 8: 61499-509.

10. De-Ugarte L, Yoskovitz G, Balcells S, et al. MiRNA profiling of whole trabecular bone: identification of osteoporosis-related changes in MiRNAs in human hip bones. BMC Med Genomics 2015; 8: 75.

11. Li H, Yu L, Liu J, et al. miR-320a functions as a suppressor for gliomas by targeting SND1 and beta-catenin, and predicts the prognosis of patients. Oncotarget 2017; 8: 19723-37.

12. Zhu H, Jiang X, Zhou X, et al. Neuropilin-1 regulated by miR-320 contributes to the growth and metastasis of cholangiocarcinoma cells. Liver Int 2018; 38: 125-35.

13. Song Y, Liu X, Feng X, et al. NRP1 accelerates odontoblast differentiation of dental pulp stem cells through classical Wnt/beta-catenin signaling. Cell Reprogram 2017; 19: 324-30.

14. Li Z, Hao J, Duan X, et al. The role of semaphorin 3A in bone remodeling. Front Cell Neurosci 2017; 11: 40.

15. Hayashi M, Nakashima T, Taniguchi M, Kodama T, Kumanogoh A, Takayanagi H. Osteoprotection by semaphorin 3A. Nature 2012; 485: 69-74.

16. Sugiura F, Kitoh H, Ishiguro N. Osteogenic potential of rat mesenchymal stem cells after several passages. Biochem Biophys Res Commun 2004; 316: 233-9.

17. Huang C, Li S. Correlation research between osteoporosis and left ventricular hypertrophy in older men. Arch Med Sci 2016; 12: 1220-4.

18. Gupta RA, Shah N, Wang KC, et al. Long non-coding RNA HOTAIR reprograms chromatin state to promote cancer metastasis. Nature 2010; 464: 1071-6.

19. Tong X, Gu PC, Xu SZ, Lin XJ. Long non-coding RNA-DANCR in human circulating monocytes: a potential biomarker associated with postmenopausal osteoporosis. Biosci Biotechnol Biochem 2015; 79: 732-7.

20. Zuo C, Wang Z, Lu H, Dai Z, Liu X, Cui L. Expression profiling of lncRNAs in C3H10T1/2 mesenchymal stem cells undergoing early osteoblast differentiation. Mol Med Rep 2013; 8: 463-7.

21. Ying G, Bo L, Yanjun J, Lina W, Binquan W. Effect of a local, one time, low-dose injection of zoledronic acid on titanium implant osseointegration in ovariectomized rats. Arch Med Sci 2016; 12: 941-9.

22. Xiao X, Zhou T, Guo S, et al. LncRNA MALAT1 sponges miR-204 to promote osteoblast differentiation of human aortic valve interstitial cells through up-regulating Smad4. Int J Cardiol 2017; 243: 404-12.

23. He L, Hannon GJ. MicroRNAs: small RNAs with a big role in gene regulation. Nat Rev Genet 2004; 5: 522-31.

24. Mohajeri M, Banach M, Atkin SL, et al. MicroRNAs: novel molecular targets and response modulators of statin therapy. Trends Pharmacol Sci 2018; 39: 967-81.

25. Michalska-Kasiczak M, Bielecka-Dabrowa A, von Haehling S, Anker SD, Rysz J, Banach M. Biomarkers, myocardial fibrosis and co-morbidities in heart failure with preserved ejection fraction: an overview. Arch Med Sci 2018; 14: 890-909.

26. Momtazi AA, Banach M, Pirro M, Stein EA, Sahebkar A. MicroRNAs: new therapeutic targets for familial hypercholesterolemia? Clin Rev Allergy Immunol 2018; 54: 224-33.

27. Taipaleenmaki H. Regulation of bone metabolism by microRNAs. Curr Osteoporos Rep 2018; 16: 1-12.

28. Hackl M, Heilmeier U, Weilner S, Grillari J. Circulating microRNAs as novel biomarkers for bone diseases –

complex signatures for multifactorial diseases? Mol Cell Endocrinol 2016; 432: 83-95.

29. Salmena L, Poliseno L, Tay Y, Kats L, Pandolfi PP. A ceRNA hypothesis: the Rosetta Stone of a hidden RNA language? Cell 2011; 146: 353-8.

30. Liu Y, Hu J, Liu B, Jiang X, Li Y. The effect of osteoprotegerin on implant osseointegration in ovariectomized rats. Arch Med Sci 2017; 13: 489-95.

31. Indran IR, Liang RL, Min TE, Yong EL. Preclinical studies and clinical evaluation of compounds from the genus Epimedium for osteoporosis and bone health. Pharmacol Ther 2016; 162: 188-205.

32. Nakamura A, Dohi Y, Akahane M, et al. Osteocalcin secretion as an early marker of in vitro osteogenic differentiation of rat mesenchymal stem cells. Tissue Eng Part C Methods 2009; 15: 169-80.

33. Baron R, Kneissel M. WNT signaling in bone homeostasis and disease: from human mutations to treatments. Nat Med 2013; 19: 179-92.

34. Chen Y, Whetstone HC, Lin AC, et al. Beta-catenin signaling plays a disparate role in different phases of fracture repair: implications for therapy to improve bone healing. PLoS Med 2007; 4: e249.

35. Li H, Yu L, Liu J, et al. miR-320a functions as a suppressor for gliomas by targeting SND1 and beta-catenin, and predicts the prognosis of patients. Oncotarget 2017; 8: 19723-37.